Growth of large-sized graphene thin-films by liquid precursor-based chemical vapor deposition under atmospheric pressure

Xiaochen Dong[1], Peng Wang[1], Wenjing Fang[3], Ching-Yuan Su[4], Yu-Hsin Chen[4], Lain-Jong Li[4], Wei Huang[1], Peng Chen[2],*

[1] *Key Laboratory for Organic Electronics & Information Displays (KLOEID), Institute of Advanced Materials (IAM), Nanjing University of Posts and Telecommunications (NUPT), 9 Wenyuan Road, Nanjing 210046, China*

[2] *School of Chemical and Biomedical Engineering, Nanyang Technological University, Singapore, 637459*

[3] *School of Materials Science and Engineering, Nanyang Technological University, Singapore, 639798*

[4] *Research Center for Applied Sciences, Academia Sinica, Taipei 11529, Taiwan*

Abstract:

Large-sized thin-films composed of single- and few-layered graphene have been synthesized by chemical vapor deposition (CVD) on copper foils under atmospheric pressure using ethanol or pentane as the precursor. Confocal Raman measurements, transmission electron microscopy and scanning tunneling microscopy show that the majority part of the obtained films exhibit hexagonal graphene lattice. Optical microscopy and electrical measurements confirm the continuity of these films. It is also found that the CVD- grown graphene

*corresponding authors: Tel: +65 65141086 (P Chen)
E-mail addresses: chenpeng@ntu.edu.sg (P Chen)

films with ethanol as the precursor exhibit lower defect density, higher electrical conductivity, and higher hall mobility than those grown with pentane as the precursor. This liquid-precursor-based atmospheric-pressure CVD synthesis provides a new route for simple, inexpensive and safe growth of graphene thin-films.

1. Introduction

Graphene, a single layer of carbon atoms bonded into a two-dimensional hexagonal crystal structure, has attracted a great deal of attention since its discovery in 2004 [1]. Graphene possesses extraordinary physical and electrical properties including quantum-spin Hall effect [2], quasiparticle coupling [3], extremely high mobility [4], and electromechanical response [5]. The unique properties of graphene have sparked tremendous interest in its potential for future electronics such as high-speed and radio frequency devices [6], nanoelectronics [7], and bioelectronics [8, 9]. Also, graphene films can serve as transparent electrode materials [10] in solar cells [11], liquid crystal devices [12] and ultracapacitors [13].

To realize these applications, the reproducible and readily fabrication of large-scale graphene film with high quality is of obvious importance. Various approaches have been developed to produce single or few-layer graphene, such as mechanical exfoliation from graphite [14], epitaxial growth [15-16], chemical exfoliation [17], chemical reduction of graphene oxides [18-21], and chemical vapor deposition (CVD) [22-24]. Among them, the CVD growth is particularly advantageous for the preparation of large area and high quality graphene film. Reina et al. have demonstrated that single- and few-layered graphene films can be synthesized on the surface of polycrystalline Ni by CVD using methane as the precursor (carbon source) [25]. Recent reports have shown that the large-area graphene films can also

grow on copper foil using CVD [26]. All these CVD growth methods rely on methane gas as the precursors and low pressure conditions. Methane is extremely flammable and may form explosive mixtures with air. Therefore, seeking for a benign alternative is much desired. Recently, Srivastava et al. reported that continuous graphene film can be CVD-grown using hexane as the precursor under low pressure condition [27]. Here we report the CVD growth of continuous, single- and few-layered graphene films on copper foils with ethanol or pentane liquid as the precursor under atmospheric pressure (APCVD).

2. Experimental Section

2.1 *Growth of graphene with liquid precursors*

Copper foils (50 μm thick; purchased from Alfa Aestar) were used as the catalytic substrates. Copper foils were loaded into a quartz tubular furnace and the quartz tube was then purged with pure Argon (1000 sccm) for 10 minutes, following by ramping up the furnace temperature to 900^{o}C in hydrogen/argon (H_2/Ar) environment (20% H_2; 100 sccm). After the temperature reached 900^{o}C, the H_2/Ar environment was maintained for 10 minutes to reduce the native copper oxide on the surface of copper foils. The APCVD growth of graphene was started by flowing H_2/Ar gas mixture (20% H_2; 40 sccm) through the liquid precursor to the furnace. During the growth stage, the additional 1000 sccm of Ar was introduced to dilute the concentration of the organic precursors brought in by H_2/Ar. The growth time was about 30 minutes. The schematic APCVD setup for graphene growth is shown in Fig. 1. After CVD growth, the copper foils in the quartz tube were cooled down under the H_2/Ar environment.

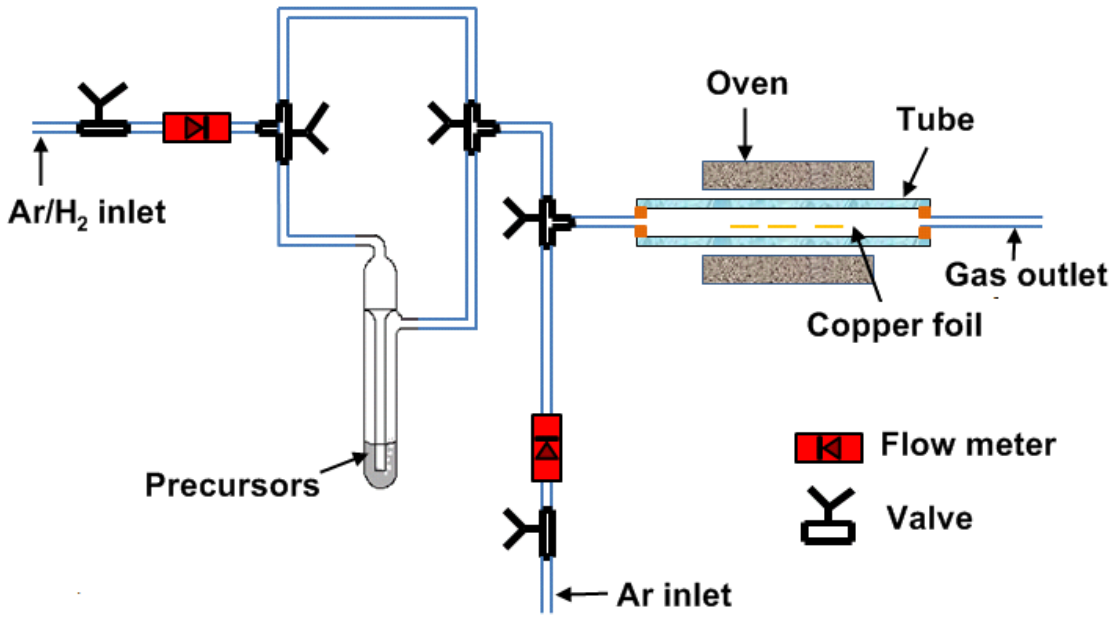

Fig. 1. Schematic of APCVD setup for graphene growth using organic liquid as the precursor. In the process of graphene film growth, vapor of the organic liquid precursor was brought into the reaction tube as Ar/H_2 gas mixture bubbled through the liquid precursor.

2.2 *Transfer of as-grown graphene films*

A thin layer of poly(methyl methacrylate) (PMMA) was spin-coated on top of obtained graphene films on copper foils. After coating PMMA, the sample was annealed at 180^{o}C in ambient for 1minute. The graphene/PMMA films were then released from the copper foil by chemical etching of the underlying Cu in an iron chloride solution. The suspended films were transferred to deionized water to remove the residual copper etchant. Subsequently, graphene/PMMA films were transferred onto desired substrates, such as Si/SiO_2. Finally, the PMMA films were dissolved by acetone and the samples were rinsed with DI-water.

2.3 *Characterization of graphene films*

Optical microscopy and tapping-mode atomic force microscopy (AFM) were used to examine the surface morphology of graphene films on Si/SiO_2 substrate (300 nm thick SiO_2). Raman

spectra were obtained with a WITec CRM200 Confocal Raman microscopy system (laser wavelength 488 nm and laser spot size about 0.5 mm); the Si peak at 521 cm^{-1} was used as a reference for wavenumber calibration. Transmission electron microscopy (JEOL JEM-2010) was operated at an accelerating voltage of 200 kV. Scanning Tunneling Microscopy (STM) analysis of the as-grown graphene films were carried out on a Veeco STM base in ambient condition. The measurement of hall mobility and sheet resistance was performed in ambient with a magnetic field (6800G) based on the Van der Pauw method [28], where the sample size for the Hall effect measurement is ~0.6 cm × 0.6 cm.

To evaluate the electrical properties of the devices made from the synthesized graphene films, bottom-gated graphene-based field effect transistors (FETs) were fabricated. The as-grown graphene films were transferred onto SiO_2/Si substrate, and then covered with a copper grid (as a hard mask). The Au source and drain electrodes (30 nm thick) were subsequently deposited on top of the graphene layer by thermal evaporation. All electrical measurements were performed in ambient condition using a Keithley semiconductor parameter analyzer (model 4200-SCS).

3. Results and Discussion

The optical image for a typical graphene film grown with ethanol and transferred on 300 nm SiO_2/Si substrate is shown in Fig. 2a. It is evident that large area and continuous graphene film was obtained with certain inhomogeneity in film thickness. Dark blue patches are multilayered graphene [29]. The light blue regions in the optical micrograph correspond to the single- or double-layered graphene films (Fig. 2a). The thickness of these regions is about 1.50 nm as measured by AFM (inset of Fig. 2b). The thickness of the dark blue regions is about 2~6 nm. Approximately, the graphene film is composed of ~ 50-60 % single- or

double-layered graphene. Fig. 2b shows the AFM image of a typical graphene film obtained using ethanol as the precursor. The height profile demonstrates the uniformity of the graphene film. However, some wrinkles (~4-8 nm in height) are also observed. These are likely formed during the cooling stage due to the difference in the thermal expansion coefficients between the metal foil and the as-grown graphene film [30, 31]. The transfer process from Cu to SiO_2 may also produce some wrinkles. There are some bright dots seen on the surface of graphene, corresponding to a height of about 25 nm. These may be the PMMA residuals.

Raman spectroscopy is instrumental for characterization of graphene structure, defects and thickness. Fig. 2c shows the typical Raman spectra of single-, double- and multi-layered graphene films detected at selected locations of the graphene films grown with ethanol as the precursor. The Raman spectra indicate that the CVD-grown graphene films exhibit G and 2D peaks at ~1575 and ~2700cm^{-1} regardless of their thickness, which is consistent with the literature [32]. The D band is observed at ~1350cm^{-1}, suggesting the presence of disordered structural defects (e.g., amorphous carbon or edges that break the symmetry and selection rule) [33]. For the single-layered graphene, the 2D band is narrow (full-width at half-maximum ~20.50 cm^{-1}, which is calculated with respect to a baseline obtained by drawing a tangent line to the spectrum between 2600 and 2800cm^{-1}). The ratio of the peak area of 2D and G bands (I_{2D}/I_G) is about 2.10 and the ratio of the peak area of D and G band (I_D/I_G) is about 0.23. Double- and multi-layered graphene exhibit significantly larger peak width (full-width at half-maximum from ~27.70 to 43.80 cm^{-1}) compared with the single-layered graphene. Thus, the Raman mapping of the APCVD-grown graphene film grown with ethanol (Fig. 2d), which is constructed by plotting peak width of the 2D-band (2600-2800cm^{-1}) as the map height, allows us to identify the thickness of the graphene films at a specific location

(spatial resolution is limited by the optical limit of the Raman system ~ 0.5 μm). As seen from Fig. 2a, the domain size of single-layered graphene in the film typically reaches 2×2 μm in size.

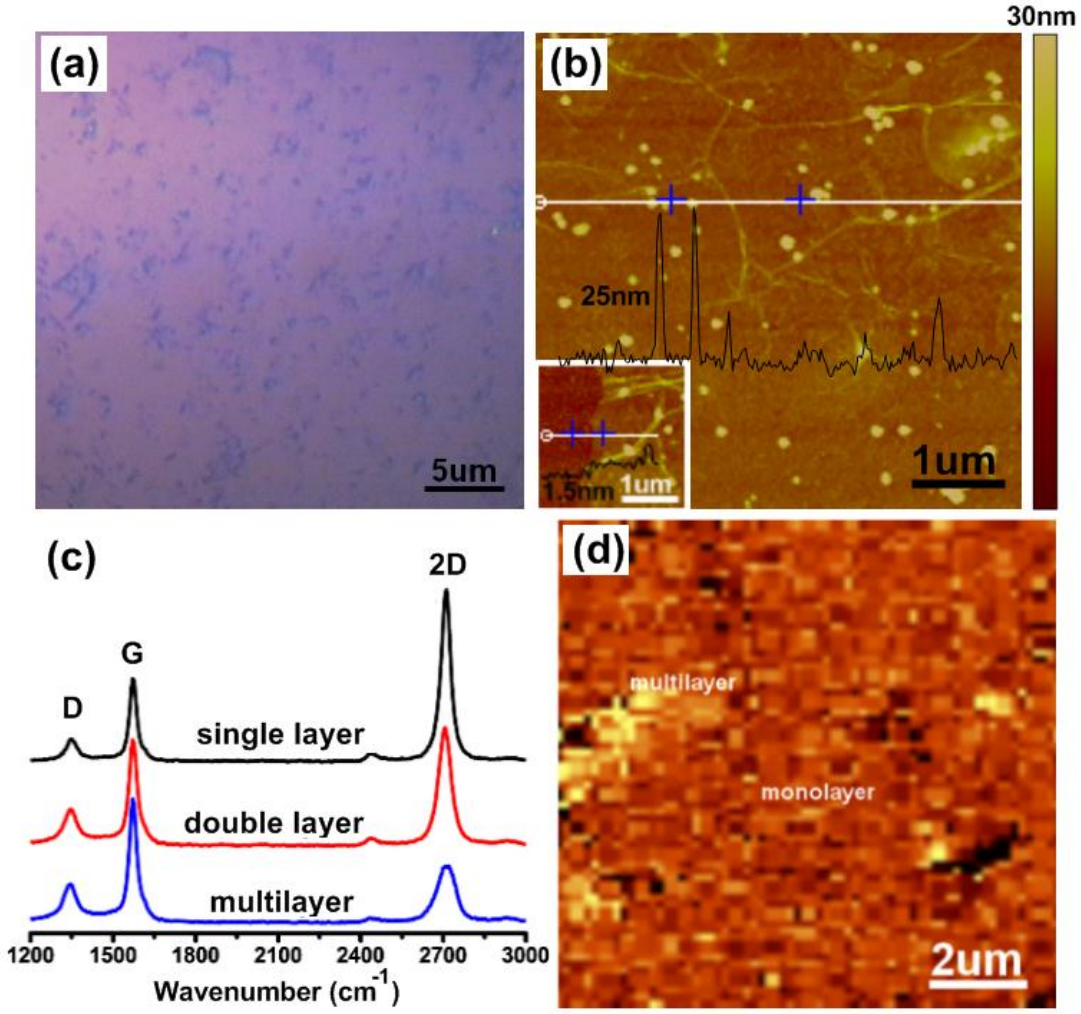

Fig. 2 APCVD-grown graphene films with ethanol as the precursor. (a) Optical micrograph of the obtained graphene films on Si/SiO_2 substrate. (b) AFM image of the graphene film on Si/SiO_2 substrate. The inset shows that the thickness of the selected film edge is around 1.5 nm. (c) Raman spectra of single-, double-and multi-layered graphene. (d) Raman map of the graphene film. This map is constructed by plotting peak width of the 2D-band (2600-2800 cm^{-1}) as the map height.

The CVD grown graphene films were transferred to lacey carbon-coated grids and examined by transmission electron microscope (TEM). As shown in Fig. 3, single, triple, or a few layered graphene films can be identified. This is consistent with the Raman characterizations.

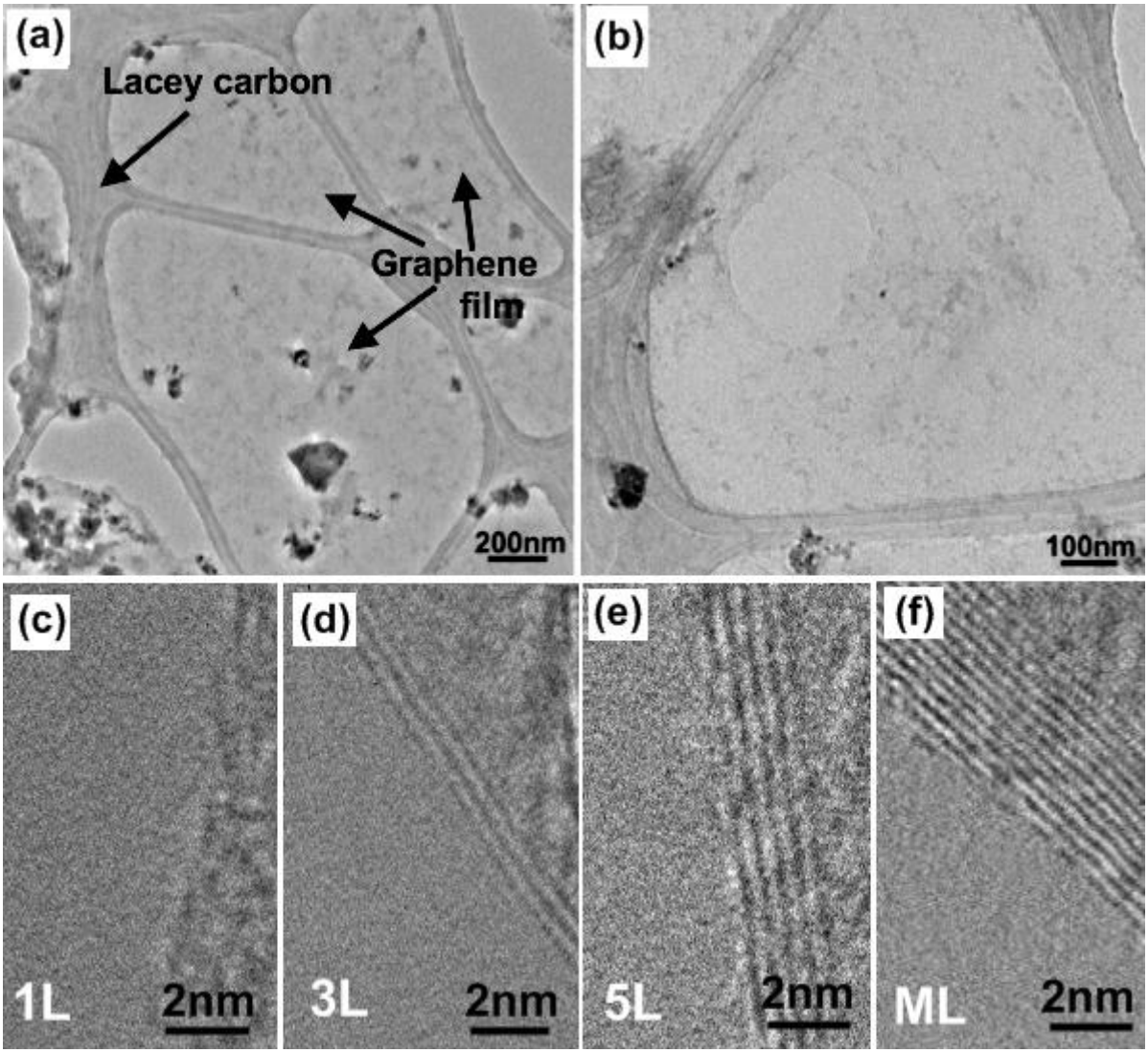

Fig. 3. TEM images of the CVD grown graphene films using ethanol as the precursor. (a, b) Low-magnification TEM images of graphene films. (c-f) High-magnification TEM image of graphene showing the edges of the film containing one (c), three (d), five (e), and multi- (f) layers of graphene film. The cross-sectional view is enabled by tilting the samples by 24 degrees.

The synthesis of graphene films using another precursor pentane was also performed. For comparison, all the parallel characterization results for this type of film were shown in Fig. 4. The optical micrograph shown in Fig. 4a suggests that such graphene film is also continuous in a large area but the thickness of the graphene film is not as homogenous as those grown using ethanol as the precursor. The AFM image in Fig. 4b also indicates that the surface of graphene film grown from pentane is rougher than that grown from ethanol. In addition to the wrinkles, some large and irregular-shaped particles are also observed. We believe that these particles are thick multilayered graphene and some impurities (such as amorphous carbon) formed during the CVD growth process. Similar to the graphene grown by ethanol, the single-layered pentane grown graphene has sharp and narrow 2D peak (full-width at half-maximum ~20.80 cm^{-1}) (Fig. 4c). However, its D band at ~1350 cm^{-1} is more pronounced. And there is a weak D' peak at ~1630cm^{-1} and the I_D/I_G ratio is about 0.66, which is larger than that of graphene grown by ethanol. All these Raman signatures suggest that the graphene films grown by pentane possess more defects comparing with those grown by ethanol. And both AFM and Raman results show that the graphene films grown with pentane are not uniform in thickness. In general, the APCVD graphene grown by ethanol is more uniform and clean. This is likely due to that the oxygen species resulting from the thermal decomposition of ethanol can etch the amorphous carbon during the CVD growth process [34-36].

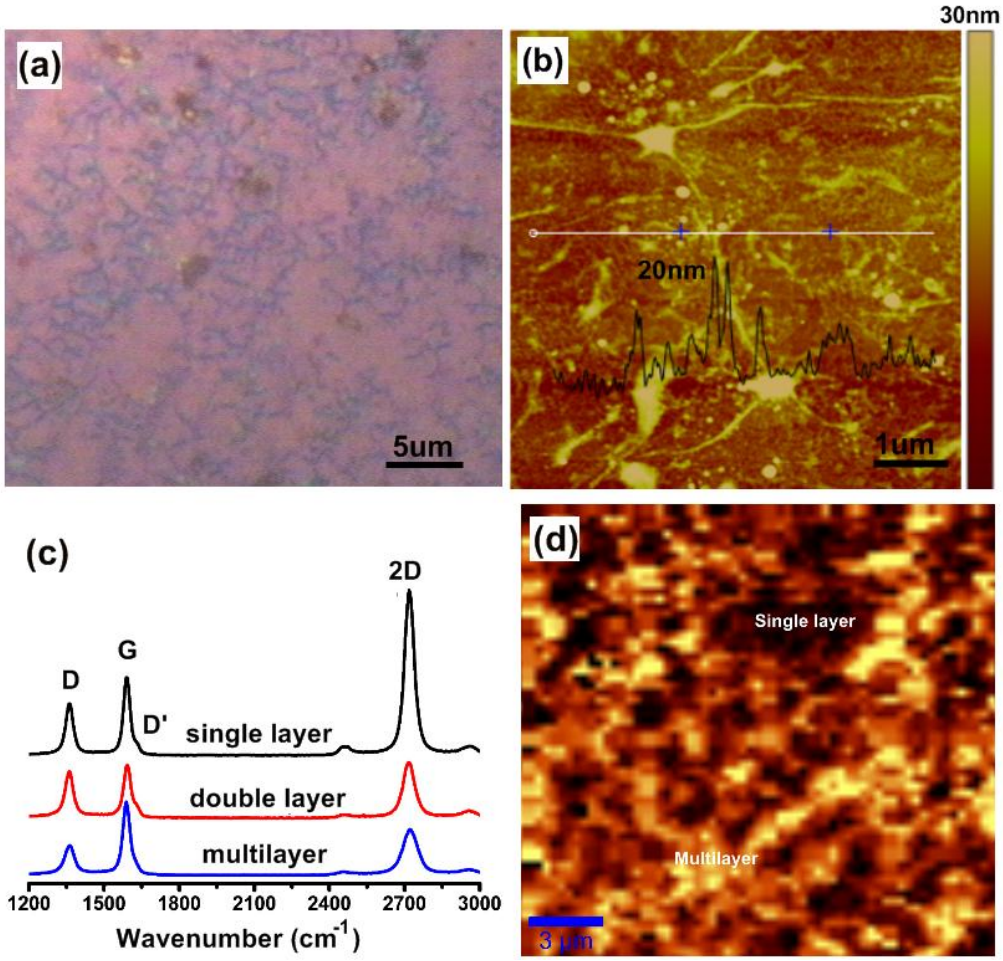

Fig. 4 APCVD-grown graphene films with pentane as a precursor. (a) Optical micrograph of the obtained graphene films on Si/SiO_2 substrate. (b) AFM image of the graphene film on Si/SiO_2 substrate. (c) Raman spectra of single-, double-and multi-layered graphene. (d) Raman map of the graphene film. This map is constructed by plotting peak width of the 2D-band (2600-2800cm^{-1}) as the map height.

To reveal the structure of graphene films grown with ethanol and pentane, these as-grown graphene films on the Cu foils were characterized with STM, as shown in Fig. 5a and 5c. To filter out the unwanted signal from Cu substrate and noises from the measurement, we performed the Fourier transform (FT) for the obtained real space STM image and we selected the desired periodic pattern from the obtained k-space image. After reverse FT for the

selected k-space image, we obtain corrected STM images for the graphene film, as shown in Fig. 5b and 5d respectively. These STM images confirm the hexagonal carbon lattice of graphene [37]. Many of our STM images show that, in general, more ordered hexagonal lattice (with less defects) was observed for the graphene films grown by ethanol. These STM results agree with the conclusions drawn from the Raman spectra and AFM images, i.e., the graphene films grown by ethanol are of better quality than those grown by pentane.

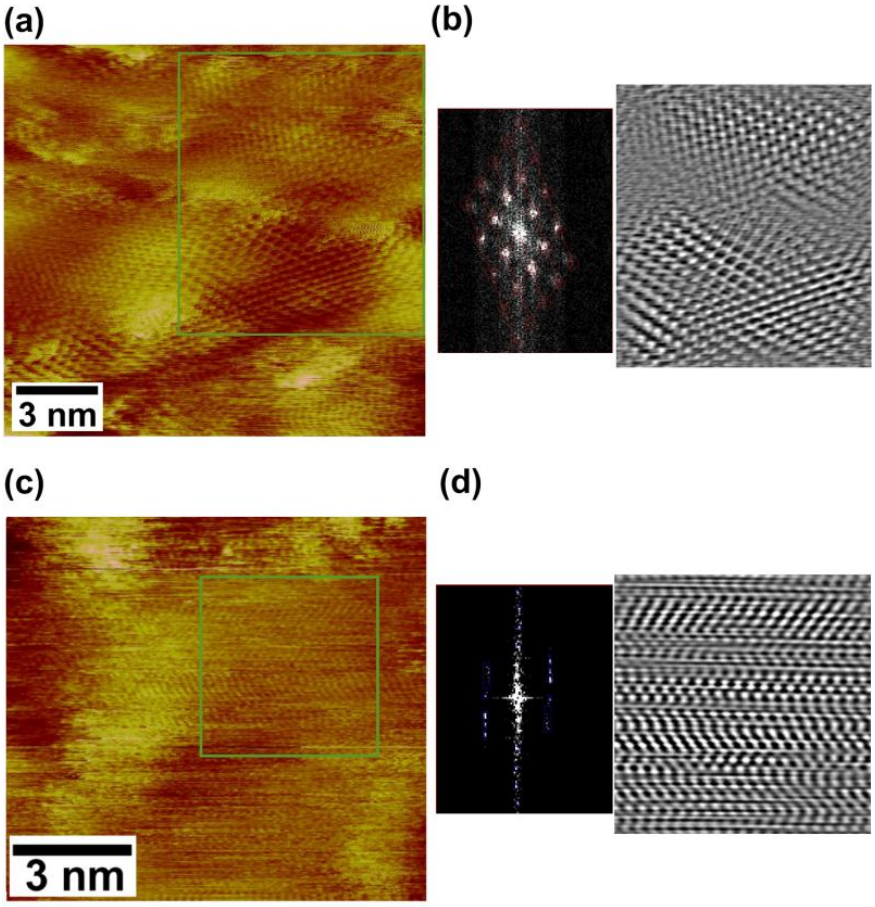

Fig. 5. (a) STM images of CVD-grown graphene film using ethanol as the precursor. (b) The left graph shows the k-space image of the squared area indicated in (a), and the right graph shows the STM image after reverse Fourier transform (FT) for the k space image after selecting circled periodic points as indicated. (c) STM images of CVD-grown graphene film using pentane as the precursor. (d) The corresponding k-space and reverse FT images for the indicated area in (c).

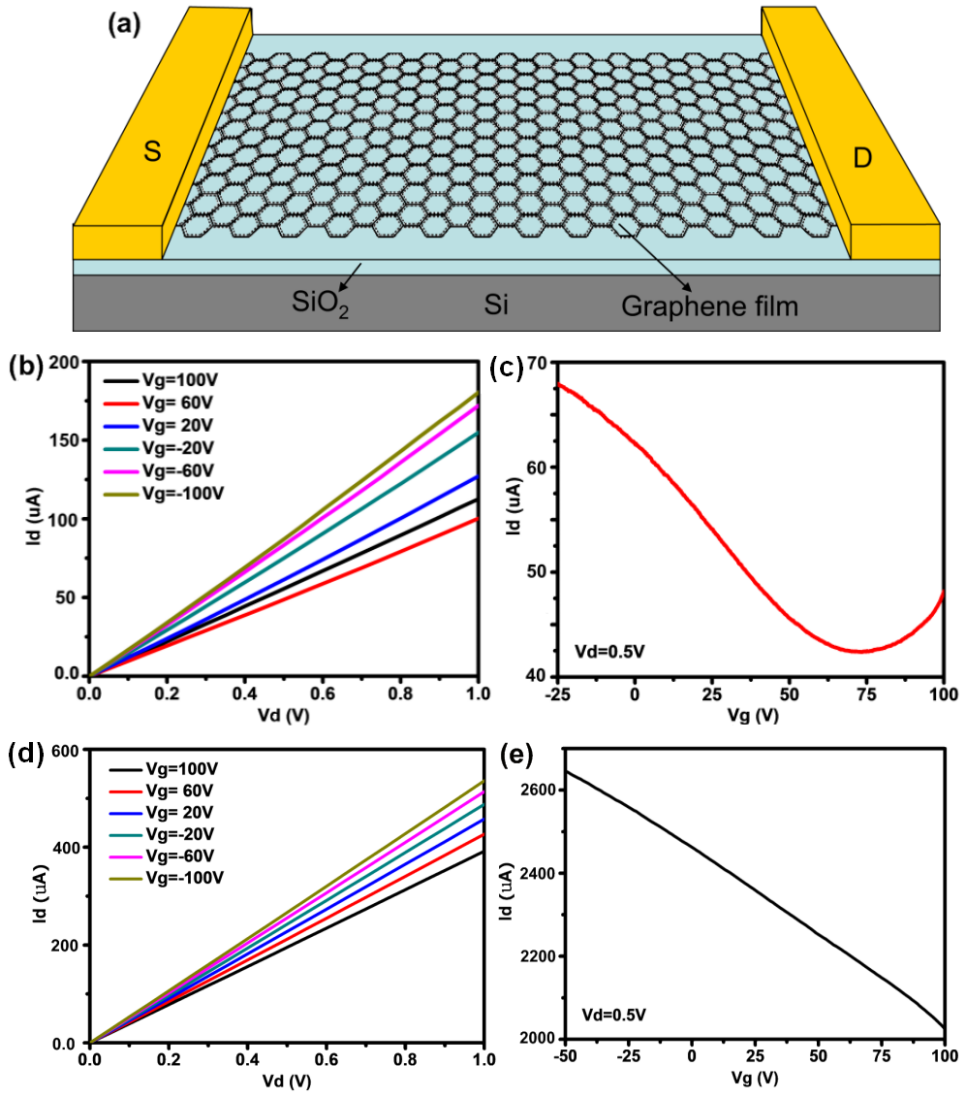

Fig. 6. (a) Shcematic illustration of the graphene transistor device. (b) I_d-V_d curves of graphene transistor at different V_g (ethanol as the precursor). (c) I_d-V_g curves of graphene transistors at V_d = 0.5V (ethanol as the precursor). (d) I_d-V_d curves of graphene transistors at different V_g (pentane as the precursor). (e) I_d-V_g curves of graphene transistors at V_d = 0.5V (pentane as the precursor).

To study the electrical properties of the transistor devices made from the two types of CVD grown graphene films, the field-effect transistors were fabricated as described in the experimental section. The schematic illustration for the transistor device is shown in Fig. 6a.

Both ethanol grown and pentane grown graphene films exhibit linear drain current (I_d) and drain voltage (V_d) relation (Fig. 6b and 6d). The transfer curve (drain current I_d vs back-gate voltage V_g) of ethanol-grown graphene shows ambipolar characteristics with the neutrality point at about 70V (Fig. 6c). Its on/off ratio is about 1.50, similar to that observed from pristine single-layered graphene by mechanical exfoliation [38]. By contrast, the I_d-V_g curve of the device fabricated with pentane-grown graphene film presents only p-type conductance and weak dependence on gate voltage when V_g is swept from 100V to -50V (Fig. 6e). No neutrality point is observed, similar to the previously reported low-pressure CVD-grown graphene films with hexane as the precursor [27]. It may be attributable to the fact that the pentane-grown graphene films are not uniform in thickness and the thick multilayered graphene and the defects may dominate the electrical properties of the films.

We have also measured the sheet resistance and hall mobility of the resulting large-sized graphene films, as shown in Table 1. The results indicate that the hall mobility of ethanol growth graphene film can reach 110 cm^2/Vs and is similar to the graphene films grown with methane gas as the precursor (100-2000cm^2/Vs) [25]. And it is higher than that of pentane-grown graphene films (64.8 cm^2/Vs). In addition, the ethanol grown graphene films have higher conductivity. It is likely that the electrical properties of pentane grown graphene films are largely impaired by their defects and abnormal morphology.

Table 1. Sheet resistance and hall mobility of APCVD-grown graphene films.

Precursors	R_S(ohm/sq)	Hall mobility(cm^2/Vs)
Ethanol	2657±960	110.4±8.8
Pentane	4989±940	64.8±27

4. Conclusions

We have obtained large-sized, continuous, thin graphene films by CVD on the surface of copper foils under atmospheric pressure, with liquid ethanol or pentane as the precursor. AFM, Raman, TEM and STM measurements indicate that the ethanol grown graphene films possess lower defect density, better hexagonal carbon lattice and better uniformity as compared with those grown by pentane. Therefore, the ethanol grown graphene films exhibit better electrical properties, specifically, ambipolar field-effect, lower sheet resistance and higher hall mobility. This APCVD growth with organic precursors provides a new, simple and safe route for the preparation of large-scale graphene films with single or a few layers. This development may provide a thrust to the development of practical graphene devices such as cheap flexible electronics.

Acknowledgements

We acknowledge the financial support from the NNSF of China (50902071, 61076067), the 973 Program (China, 2009CB930601), the Science Foundation of Nanjing University of Posts and Telecommunications (NY208058), the Research Center for Applied Science (Academia Sinica, Taiwan), A-Star SERC grant (No. 072 101 0020, Singapore) and National Research Foundation Singapore (NRF- CRP 2-2007-02).

References

[1] Novoselov KS, Geim AK, Morozov SV, Jiang D, Zhang Y, Dubonos SV, et al. Electric field effect in atomically thin carbon films. Science 2004; 306, 666-669.

[2] Zhang Y, Tan YW, Stormer HL, Kim P, Experimental observation of the quantum Hall

effect and Berry's phase in graphene. Nature 2005; 438, 201-204.

[3] Bostwick A, Ohta T, Seyller T, Horn K, Rotenberg E. Quasiparticle dynamics in graphene. Nature Phys 2007; 3, 36-40.

[4] Bolotin KI, Sikes KJ, Jiang Z, Klima M, Fudenberg GJ, Honec PK, et al. Ultrahigh electron mobility in suspended graphene. Solid State Commun 2008; 146, 351-355.

[5] Bunch JS, Zande AM, Verbridge SS, Frank IW, Tanenbaum DM, Parpia JM, et al. Electromechanical resonators from graphene sheets. Science 2007; 315, 490-493.

[6] Lin YM, Dimitrakopoulos C, Jenkins KA, Farmer DB, Chiu HY, Grill A. 100-GHz transistors from wafer-scale epitaxial graphene. Science 2010; 327, 662.

[7] Schwierz F. Graphene transistors. Nature Nanotechnol 2010; 5, 487-496.

[8] Dong XC, Shi YM, Huang W, Chen P, Li LJ, Electrical detection of DNA hybridization with single-base specificity using transistors based on CVD-grown graphene sheets. Adv Mater 2010; 22, 1649-1653.

[9] Huang YX, Dong XC, Shi YM, Li CM, Li LJ, Chen P. Nanoelectronic biosensors based on CVD grown graphene. Nanoscale 2010; 2, 1484-1488.

[10] Kim KS, Zhao Y, Jang H, Lee SY, Kim JM, Kim KS, et al. Large-scale pattern growth of graphene films for stretchable transparent electrodes. Nature 2009; 457, 706-710.

[11] Wang X, Zhi L, Müllen K. Transparent, conductive graphene electrodes for dye-sensitized solar cells. Nano Lett 2008; 8, 323-327.

[12] Blake P, Brimicombe PD, Nair RR, Booth TJ, Jiang D, Schedin F, et al. Graphene-based liquid crystal device. Nano Lett 2008; 8, 1704-1708.

[13] Stoller M, Park S, Zhu Y, An J, Ruoff R. Graphene-based ultracapacitors. Nano Lett 2008; 8, 3498-3502.

[14] Dong XC, Fu DL, Fang WJ, Shi YM, Chen P, Li LJ. Doping single-layer graphene with aromatic molecules. Small 2009; 5, 1422-1426.

[15] Berger C, Song Z, Li T, Li X, Feng R, Dai Z, et al. Ultrathin epitaxial graphite: 2D electron gas properties and a route toward graphene-based nanoelectronics. J. Phys. Chem. B 2004; 108, 19912-19916.

[16] Berger C, Song Z, Li X, Wu X, Brown N, Naud CC, et al. Electronic confinement and coherence in patterned epitaxial graphene. Science 2006; 312, 1191-1196.

[17] Dong XC, Shi YM, Zhao Y, Chen DM, Ye J, YaoYG, et al. Symmetry breaking of graphene monolayer by moleculat decoration. Phys Rev Lett 2009; 102, 135501-135504.

[18] Dikin DA, Stankovich S, Zimney EJ, Piner RD, Dommett GHB, Evmenenko G, et al. Preparation and characterization of graphene oxide paper. Nature 2007; 448, 457-460.

[19] Dong XC, Su CY, Zhang WJ, Zhao JW, Ling QD, Huang W, et al. Ultra-large single-layer graphene obtained from solution chemical reduction and its electrical properties. Phys Chem Chem Phys 2010; 12, 2164-2169.

[20] Kim JY, Cote LJ, Kim F, Yuan W, Shull KR, Huang JX. Graphene oxide sheets at interfaces. J. Am. Chem. Soc. 2010; 132, 8180-8186.

[21] Cote LJ, Kim F, Huang JX. Langmuir-Blodgett assembly of graphite oxide single layers. J. Am. Chem. Soc. 2009; 131, 1043-1049.

[22] Sutter PW, Flege JI, Sutter EA. Epitaxial graphene on ruthenium. Nature Mater 2008; 7, 406-411.

[23] Kwon SY, Ciobanu CV, Petrova V, Shenoy VB, Bareno J, Gambin V, et al. Growth of semiconducting graphene on palladium. Nano Lett 2009; 9, 3985-3990.

[24] Coraux J, N'Diaye AT, Busse C, Michely T. Structural coherency of graphene on Ir(111).

Nano Lett 2008; 8, 565-570.

[25] Reina A, Jia X, Ho J, Nezich D, Son H, Bulovic V, et al. Large area, few-layer graphene films on arbitrary substrates by chemical vapor deposition. Nano Lett 2009; 9, 30-35.

[26] Li XS, Cai WW, An J, Kim S, Nah J, Yang DX, et al. Large-area synthesis of high-quality and uniform graphene films on copper foils. Science 2009; 324, 1312-1314.

[27] Srivastava A, Galande C, Ci LJ, Song L, Rai C, Jariwala D,et al. Novel liquid precursor-based facile synthesis of large area continuous, single, and few-layer graphene films. Chem Mater 2010; 22, 3457-3461.

[28] Van der Pauw LJ. A method of measuring specific resistivity and Hall effect of discs of arbitrary shape. Philips Research Reports 1958; 13, 1-9.

[29] Ni ZH, Wang HM, Kasim J, Fan HM, Yu T, Wu YH,et al. Graphene thickness determination using reflection and contrast spectroscopy. Nano Lett 2007; 7, 2758-2763.

[30] Chae SJ, Gunes F, Kim KK, Kim EG, Han GH, Kim SM, et al. Synthesis of large-area graphene layers on poly-nickel substrate by chemical vapor deposition: wrinkle formation. Adv Mater 2009; 21, 2328-2333.

[31] Juang ZY, Wu CY, Lu AY, Su CY, Leou KC, Chen FR, et al. Graphene synthesis by chemical vapor deposition and transfer by a roll-to-roll process. Carbon 2010; 48, 3169-3174.

[32] Wang YY, Ni ZH, Yu T, Shen ZX, Wang HM, Wu YH, et al. Raman studies of monolayer graphene: the substrate effect. J Phys Chem C 2008; 112, 10637-10640.

[33] Ferrari AC, Meyer JC, Scardaci V, Casiraghi C, Lazzeri M, Mauri F, et al. Raman spectra of graphene and graphene layers. Phys Rev Lett 2006; 97**,** 187401-4.

[34] Hata K, Futaba DN, Mizuno K, Namai T, Yumura M, Lijima S. Water-assisted highly efficient synthesis of impurity-free single-walled carbon nanotubes. Science 2004; 306, 1362-

1364.

[35] Zhu LB, Xiu YH, Hess DW, Wong CP. Aligned carbon nanotube stacks by water-assisted selective etching. Nano Lett 2005; 5, 2641-2645.

[36] Zhang GY, Mann D, Zhang L, Javey A, Li YM, Yenilmez E, et al. Ultra-high-yield growth of vertical single-walled carbon nanotubes: hidden roles of hydrogen and oxygen. PNAS 2005; 102, 16141-16145.

[37] Hofrichter J, Szafranek BN, Otto M, Echtermeyer TJ, Baus M, Majerus A, et al. Synthesis of graphene on silicon dioxide by a solid carbon source. Nano Lett 2010; 10, 36-42.

[38] Shi YM, Dong XC, Chen P, Wang JL, Li LJ. Effective doping of single-layer graphene from underlying SiO_2 substrates. Phys Rev B 2009; 79, 115402-115404.